E7.4-10.456
CR-137445

(E74-10456) OPTICAL DATA PROCESSING ANALYSIS OF STREAM PATTERNS EXHIBITED ON ERTS-1 IMAGERY (Kansas Univ. Center for Research, Inc.) 19 p HC $4.00 CSCL 08H G3/13 00456 Unclas N74-21981

OPTICAL DATA PROCESSING ANALYSIS OF STREAM PATTERNS EXHIBITED ON ERTS-1 IMAGERY

Dwight Egbert, James McCauley
Fawwaz Ulaby, James McNaughton

University of Kansas Center for Research, Inc.
Remote Sensing Laboratory
Lawrence, Kansas 66045

ABSTRACT

The purpose of the investigation described in this paper has been the analysis of large-scale geologic ground patterns in Kansas using ERTS-1 imagery and optical data processing techniques. Optical spatial frequency data provide a repeatable quantitative means of specifying ground pattern characteristics.

INTRODUCTION

In satellite imagery of an area such as Kansas with low relief, subtle geologic structure and extensive land use, the geologic ground pattern that is most apparent is that caused by stream patterns. Pattern and frequency of streams are important indicators of the rock-type upon which they are developed. In addition, they are strongly influenced by geologic structure. Spatial frequency analysis of ERTS imagery lends itself to the study of drainage patterns by detecting those patterns which display a preferred orientation or spacing, and it also appears to provide an unbiased means of detecting and measuring linear patterns on most remote sensing products. The spatial frequency analysis in this investigation involves the determination of large-scale geologic and other ground pattern spatial frequency and orientational information from an optical data processing system using ERTS-1 imagery of Kansas as input*.

Kansas lies entirely within the Stable Interior and has suffered little in the way of tectonic activity since early Cambrian sediments were first deposited. The result has been the widespread deposition and preservation of sedimentary rocks ranging up to 2900 meters in thickness.

The sedimentary formations in Kansas are relatively thin and exhibit a slight but persistent westward dip at the surface. The present day streams and rivers of the state flow in a generally eastward direction from the piedmont of the Rocky Mountains to the Missouri and Mississippi rivers. This reflects the uplift and eastward tilting of much of the state which occurred with the formation of the Rocky Mountains. In traveling in a westward direction across the state, one experiences an increase in elevation and crosses the outcrops of progressively younger sedimentary rocks. Because of the westward dip and lack of other than broad gentle folds of the rock units and subsequent erosion, the sequence forms a series of eastward facing escarpments which account for most of the generally recognized physiographic regions of the state.

This work was supported by NASA Contract NAS 5-21822.

*For a discussion of other recent applications of optical spatial frequency analysis to remote sensing imagery the reader is referred to Lendaris and Stanley (1969), Steckley (1972), Andrews et al, (1972), and Gramenopoulos (1973).

The eight physiographic regions of Kansas are shown in Figure 1. In the eastern part of the state are the Osage Plains which are made up of a series of eastward-facing escarpments formed by outcrops of Pennsylvanian limestones and shales. The Flint Hills are actually a large escarpment formed by outcrops of a series of chert-bearing Permian limestones that are very resistant to erosion. The Dakota sandstone outcrops (Cretaceous) form the Smoky Hills upland in the North Central part of the state. Likewise, the Blue Hills are formed by outcrops of Upper Cretaceous limestones and chalks.

Beyond the Blue Hills lie the High Plains which are formed by the accumulation of sediments derived from the erosion of the Rocky Mountains to the west. Numerous aggrading streams swept eastward during the Tertiary carrying and depositing sand and gravel and forming a vast outwash plain. Subsequent erosion has formed the present land surface. Even younger deposits occur in the various prairies and lowlands associated with the Arkansas River. Some of these areas are covered with wind blown sand in the form of dunes, both stabilized and active. In the south-central part of the state are the Red Hills or Cimarron breaks marking the border of the High Plains in the vicinity of the Cimarron River, which together with its tributaries eroded into the red Permian siltstones and shales which underlie the High Plains in that area. The extreme northeast corner of the state was occupied by the Kansas glacier during the Pleistocene. As a result, the landscape was resculptured to some extent and the area was covered to varying depths by glacial deposits.

Areas of similar geologic composition in Kansas correlate very well with the eight physiographic regions in Figure 1. By definition, each region is characterized by a uniformity in landform development. In addition, each region can be considered a geologic region since it contains outcrops of the same dominant lithology and of the same geologic age. In many cases, any region also displays a uniform land-use pattern. Thus the selection of sample sites for spatial frequency analysis of geologic ground patterns was based on these eight physiographic-geologic regions.

Ten sample sites were selected for each of the eight geologic-physiographic regions in Figure 1 and two analyses were performed for each site, one with snow-cover and one without. The actual dates of acquisition of the images used in this study were contingent upon cloud cover and of course the presence of snow. As many as possible of the non-snow analyses were performed on images recorded during the summer and early fall of 1972. The snow-covered images were acquired during the following winter. For a few sample sites cloud free images with snow cover were not available, thus the sample set is not entirely complete.

The size of the area analyzed at each site is approximately 37 kilometers in diameter and the spacing of the sites was controlled by the size of the geologic region. Smaller regions such as the Glaciated Region were almost completely sampled; in larger regions, the sampling was more scattered. Also some sample sites cross over into neighboring states but remain in the same geologic region.

For all sample sites except one, MSS5(red) images were used in the analysis. This band was judged to contain the most information pertinent to the investigation. The lone exception is a sample site in northwest Kansas where all four MSS bands were available for analysis. This site contains an area of well-developed parallel drainage and all four bands were analyzed to determine the relative merits of each band.

Sample site center points are plotted in Figure 1 and each site has an alpha-numeric identifier. The letter refers to the geologic region in which the sample site occurs and the numbers identify the ten sample sites in that region. A snow-covered sample is assigned a number that is ten more than its non-snow counterpart. Thus in the case of "0-6" for instance, "0" refers to the Osage Plains region, "6" refers to the sixth sample site; "0-16" refers to the same sample site on a snow-covered image. The curves that result from the analysis of these samples are given the same designations. The sample site in the High Plains region which is analyzed on all four MSS bands is designated "M" in Figure 1 and the four samples and their resultant curves are designated M-4, M-5, M-6 and M-7 with the number corresponding to the ERTS band number.

OPTICAL PROCESSING SYSTEM DESCRIPTION

Frequency spectrum analysis is based on the capability of expansion of periodic functions in series form in terms of harmonically related sinusoids. That is, any periodic function, satisfying certain conditions (Papoulis, 1962), can be reproduced by a series or sum of sines and cosines. This series is known as the Fourier series, and the process of representing a periodic function by such a series is Fourier Analysis. An extension of Fourier analysis from periodic functions to non-periodic functions is possible by allowing the sum to pass to an integral. This extension results in the Fourier transform pair relating the original function to its frequency function. Stated otherwise, the Fourier transform maps a photograph's spatial (distance) transmission function from the spatial domain into the frequency domain.*

The process of Fourier analysis consists of determining the amplitude of the sine and cosine terms at each harmonic frequency. The Fourier series can be used to describe any arbitrary function and we can visualize the function as being made up of the sum of the various sinusoidal functions at the different harmonic frequencies. Further, if the value of the amplitudes in the Fourier Series are known we can speak of a function as having a high or low frequency content at any given frequency. The light intensity distribution in a diffraction pattern is a representation of the amplitudes of the harmonic terms expressed in complex exponential notation (Appendix A). Thus, by measuring this light distribution we can determine the Fourier series or Fourier Transform of the original input function. In an optical data processing system this input is a two dimensional distribution of density within a photographic image.

If there is a transmission fluctuation in the y direction as well as in the x direction on the input photograph then the resulting light intensity pattern will also show a frequency spectrum in both directions. Furthermore, any transmission variations in the photograph at any angle between the x and y directions will produce a frequency spectrum oriented at the same angle. In general the transmission distribution in a spacecraft photograph will contain variations in all directions between the x and y axes. Thus, the light intensity pattern and frequency spectrum for such a photograph will be a two dimensional distribution. For any particular pattern in this distribution the distance out from the center or the radius will describe the frequency content of the transmission function which caused this pattern. Likewise, the angular orientation of the pattern will describe the angular orientation of the transmission function in the photograph. To clarify the characteristics of two dimensional frequency spectra, three idealized apertures and their optical spectra are shown in Figure 2. It should be noted that these idealized patterns are very regular with sharp edges. However, the transmission functions encountered on any aerial or spacecraft images will be more random with less distinct boundaries. Thus, we would expect their frequency spectra to also be less ideal.

Several configurations for optical data processing systems are possible (Preston, 1972; Goodman, 1968; Shulman, 1970). The specific configuration used in this study is shown in Figure 3. The optical processor has three main elements: a laser, optics, and a Recognition Systems, Inc., Diffraction Pattern Sampling Unit (DPSU). An ERTS-1 70 mm positive transparency is used as the input. First, an area of the ERTS transparency (sample area) is illuminated by the incident laser beam after it passes through the lens. This beam is focused by the lens so that the point source produced by the spatial filter is imaged at a distance $z + f$ in front of the lens. The resulting light intensity distribution at this point is the optical Fourier transform or amplitude frequency spectrum of the portion of the ERTS image illuminated by the beam. The mathematical description of the system is given in Appendix A. Finally, the intensity distribution (frequency spectrum) of the ERTS image issampled by the DPSU.

---

*This brief introduction to Fourier analysis is designed to provide only a cursory qualitative understanding. For a more complete treatment the reader is referred to Ulaby et. al. (1973) and McCauley et. al (1974).

The DPSU consists of a 64 element photodiode array (shown in Figure 4) used to detect the light intensity incident upon each element, and electronics which amplify and digitize the output from each diode in the array. The diode array is composed of 32 wedge-shaped photodiodes and 32 annular ring photodiodes. The radius of a given light pattern in the frequency spectrum is proportional to the frequency of transmission variation on the image giving rise to the pattern. Thus, the 32 annular ring elements measure the spectrum as a function of frequency over all angles (10^{o}-170^{o}). Likewise, the 32 wedge shaped elements measure the spectrum as a function of angle over all frequencies.

The spatial frequency in the transform plane is related to other system parameters by:

$$s = r/d\lambda$$

where s = spatial frequency in transform plane

r = distance in transform plane measured from optical axis

d = distance from image transparency to detector

λ = wavelength of laser radiation

The spatial frequency obtained from this calcuation is converted to ground spatial frequency using image to ground scale. The resulting computer plotted curves are then light intensity vs. frequency and light intensity vs. angle. These are plotted in terms of ground spatial frequency in cycles per kilometer and direction in compass degrees clockwise from north.

Because of the large dynamic range of the spatial frequency curves they are plotted on a logarithmic scale. The orientation curves are plotted on a linear scale. Both curves are normalized, the frequency curve with respect to the zero frequency component and the orientation curve with respect to the maximum intensity value for the entire curve. The spatial frequency curves were further modified to enhance their ability to display features of interest. An average spatial frequency curve was calculated for the 80 non-snow sample areas. The point by point ratio between this curve and each individual spatial frequency curve was determined and these values were plotted on a linear scale. The amount of information present in the spatial frequency and orientational curves was reduced to a level which was managable in pattern classification algorithms. The resulting feature parameters will be discussed in detail in a later section.

A block diagram of the optical data processing system along with the pattern recognition portion of the system is shown in Figure 5. The diagram shows the flow of data originating with the ERTS image through the optical processing and data reduction steps to the classification algorithm resulting in geologic classification of the sample area.

For a better understanding of the optical processing system output, discussion of an example will be instructive. A portion of ERTS-1 image No. 1076-16393-5 is shown in Figure 6a. A representative area (area F-7) on this image was chosen from the samples to illustrate the steps involved in the analysis of each sample area.

The intensity distribution of the Fourier transform of the circular area in Figure 6a, as obtained with the optical data processing system, is shown in Figure 6b. This transform displays several features which can be directly related to features in the ERTS-1 image. The main feature of this transform is the very bright distribution which extends primarily vertically from the center of the transform (labeled as A.). This distribution is due to scan lines in the ERTS images. This distribution is not detected in the system, due to the detector array configuration. As shown in Figure 4 the detector has a 20^{o} dead space. The frequency spectrum resulting from the scan lines is situated in this dead space. Because of the nature of the Fourier transform, the scan lines, which appear horizontally in the image, produce an intense distribution perpendicular to them. This is because horizontal linear features are actually transmission variations in the vertical direction and visa versa. This must be kept in mind when analyzing frequency spectra.

The computer plots obtained from the intensity distribution of the transform are shown in Figure 6c. The cuve labeled as (1), obtained from the ring-shaped photodiodes, gives the spatial frequency contributions (on a logarithmic scale) due to ground features on the image. The curve labeled as (2), obtained from the wedge-shaped photodiodes, indicates the orientation of features in the sample area. Figure 6d shows the modified spatial frequency curve on a linear scale.As can be seen by comparing the two frequency curves the modification greatly enhances details.

There are two significant areas on the spatial frequency curves (6c, curve 1 and 6d). The first is located at approximately 0.4 cycle/km, and the second at approximately 1 cycle/km. As shown in the sample area in Figure 6a, a band which is light in tone extends through part of this area. This band represents the Kansas River flood plain which is an area of intensive agriculture. This band is approximately 2.5 kilometers wide (i.e it has a spatial frequency of 1/2.5 = 0.4 cycles/km) and apparently is responsible for the peak in the spatial frequency curves at 0.4 cycles/km. The higher frequency peak is evidently produced by the many narrower streams. This peak shows the advantage of the enhanced frequency curve of Figure 6d over the original. On the logarithmic scale curve only a small peak at about 1.2 cycles/km is evident. However, on the modified frequency curve two broad peaks between 1 and 2 cycles/km are seen. If these frequency peaks are indeed due to the many small streams, as discussed below, broad peaks would be expected due to a distribution of widths and spacings.

The orientational plot (6c, curve 2) also contains characteristics which can be related to ground features apparent in the sample area. There are two dominant peaks in the orientational curve. The peak labeled B at approximately 25° clockwise from north appears to result from the wide Kansas River flood plain. The flood plain is oriented approximately 20° to 25° clockwise from west in the image. As mentioned previously a linear feature in one direction on the image represents a transmission variation in the direction 90° to the linear feature. Thus, the orientation of the transmission variation due to the light tone of the flood plain is at approximately 25° clockwise from north.

The other major peak at approximately 75° clockwise from north labeled C appears to result from the general NNW-SSE orientation of the major streams in the area. Also, it is evident in Figure 6b that the orientational peak at C contains more high frequency components than does the peak at B. This is to be expected since the flood plain causing B is relatively wide resulting in a low frequency transmission variation. On the other hand the streams giving rise to C are relatively narrow creating high frequency transmission variations. Also, since there are many of these streams there will be some distribution of stream widths giving rise to a dispersion of frequencies. This example should demonstrate how the computer plots are related to the transform and how the transform is related, in turn, to the image.

GEOLOGIC PATTERNS ON ERTS IMAGERY

Use of spatial frequency analysis in the study of stream patterns should be guided by a knowledge of the manner in which stream patterns are expressed on ERTS imagery and how this expression varies from place to place in the state as a result of changing rock type, land use, climate and natural vegetation.

In Kansas, stream courses are generally expressed on ERTS imagery in four different ways:

1. Riparian Vegetation

In the eastern half of the state there are many stream valleys that support denser and higher stands of vegetation than do the surroundings uplands. Cottonwoods, willows and other trees and shrubs which require large amounts of water thrive near streams that are perennial or contain water during much of the year. Such streams are relatively easy to identify on ERTS-1 images with the MSS5 band giving the best expression. On this band, riparian vegetation generally appears much darker than surrounding fields and grasslands. In tht western half of the state the increased dryness restricts this type of vegetation to only the major perennial streams such as the Arkansas River and the lower Smoky Hill.

2. Pure Topographic Enhancement

Several areas in the state are largely uncultivated. For the most part, these are ranching areas that are covered with both natural and introduced grasses. Trees and shrubs are generally lacking even along streams in many of these areas. The absence of distractive patterns caused by fields and gross vegetation differences permit the enhancement of topography by differential illumination of slopes of varying orientation. This expression can be found on images covering the Kansas Flint Hills, as well as the Red Hills, Smoky Hills and dissected regions adjacent to larger streams in the High Plains.

Topographic enhancement of drainage patterns has a much broader application in the winter at times of deep snow cover. The snow has the effect of giving the landscape more uniform reflecting properties by masking over areas of different crop and vegetation type. As a result, slope orientation becomes more critical in determining the amount of sunlight reflected to the ERTS-sensors. The lower sun angle in the winter serves to further enhance the topography. Thus an area in which stream patterns are not normally discernible may display them fully when snow-covered.

3. Land-Use

Diverse land-use between stream valleys and uplands can often accentuate stream patterns. This can come about in a number of ways. One involves bottom land cultivation in an area of upland grazing and occurs in association with the major streams in the Flint Hills and other hilly areas, where the level fertile flood plains offer the most desirable farming areas. Another method by which land-use reflects stream patterns occurs in the western part of the state and is the opposite of the previously mentioned method. It is best displayed in the High Plains and dissected High Plains area where stream valleys are often rough and lack flood plains. In this case the level upland areas offer the most ideal conditions for cultivation. The valleys which are usually too rough or rocky for farming are used as pasture.

4. Direct Strem Expression

In some situations, the actual stream beds can be delineated on ERTS imagery. This occurs in two ways. In the eastern portion of the state the larger streams usually contain water throughout the year and can often be discerned on the MSS6 and MSS7 bands of ERTS imagery due to the low return of infrared energy from water bodies. Thus, the larger streams are often dark in comparison to the surrounding countrysides.

Actual stream beds in the western and south-central part of the state are also expressed on ERTS imagery though in a different manner. In this situation, it is the dry stream beds which give a distinctive appearance. These dry streams are choked with sand, which highly reflects energy in the visible region and produces a bright appearance on MSS4 and MSS5 images in contrast to the less bright appearance of surrounding fields and vegetation.

QUALITATIVE IMAGE ANALYSIS

In Figure 7 are the MSS 4, 5, 6 and 7 images of sample site "M" in Figure 1. This area is in the High Plains region of northwestern Kansas and contains pronounced NW-SE parallel drainage. All four MSS bands were analyzed to determine the relative merits of each in expressing this drainage alignment. The expression on ERTS imagery of this pattern is due primarily to differences in land-use between the valleys and the uplands, the uplands being level and cultivated, the valleys being rough and used as grazing land. The upland fields tend to be elongated in a N-S direction, being constrained by the topography.

Curves for the four bands are presented in Figure 7. The MSS 4 image produces a prominent peak at 100° in its orientation curve. This peak results from field patterns that are apparent on the image. The NW-SE drainage pattern is visible on the image but is secondary in importance and accounts for the peaks at 75° and 85°. The MSS 5 image produces a prominent peak at 75° in its corresponding curve that reflects the parallel drainage pattern which is quite apparent in the imagery. Field patterns are also visible but produce a secondary peak at 100°.

The MSS 6 and MSS 7 images are quite similar in appearance and produce similar curves both having sharp peaks at 100° that result from field patterns. The parallel drainage pattern is subdued on the images and likewise fails to register significantly in the resulting curves. These results substantiate our choice of MSS 5 imagery for use in this investigation because of its greater content of geological ground pattern information.

Areas F-4 (Figure 8) and F-6 (Figure 9a) are located in the Flint Hills of Kansas, and area of thin soils and moderate relief which is devoted largely to ranching, cultivation being secondary in importance. Because of the nature of the land-use in this area and the fact that trees are restricted to the larger stream valleys, drainage patterns are well displayed. Spatial frequency curves faithfully reflect those stream patterns with preferred orientations.

In Image F-4, three sets of drainage components are visible trending NW-SE,NS, and NE-SW, which account for the peaks at 40°, 90° and 160° respectively in the spatial frequency curve. The NW-SE trending drainage pattern appears to be dominant on the image, it likewise produces the strongest intensity response. A high value also occurs on the graph at 25° resulting from orientations approximately E-W. Some E-W drainage components are visible, however a major E-W highway crosses the northern part of the image and is primarily responsible for this peak.

Area F-6 is mostly rangeland with some cultivation in the valley bottoms and on the level uplands. Topographic relief is less in this area than in area F-4, however stream courses are still well defined. Three primary drainage orientations are again visible in the image; ESE, NNW-SSE, and NE, accounting for peaks at 30°, 70°, and 145° respectively in the resulting curve. The 145° peak is the strongest and corresponds to the major drainage direction. High curve values also occur at 90° and 180° that result from field and section road patterns in the cultivated areas of the images.

Image F-16 (Figure 9b) covers the same area as F-6 but was recorded after a light snowfall. Whereas a heavy snowfall has the effect of masking most vegetation and agricultural patterns, a light snow enhances them. Comparison of F-6 and F-16 makes this apparent. The snow-covered image contains numberous distracting patterns even in areas of rangeland where the thin snow cover serves to accentuate pastures with differing grass heights.

Image G-5 (Figure 10a) is a sample of the Glaciated Region of northeast Kansas. This area has a gently rolling topography and is mostly overlain by glacial deposits. Corn belt type agriculture is the dominant land use and this is apparent in the image. Fields and pastures are generally small with numerous interspersed woodlots and tree-lined streams. In addition, the section road network is very complete in this region and many are visible in the image. The result is a very complex ground pattern due to the various small image components most of which are orthogonal in nature as a result of the township and range survey system. The agricultural patterns also dominate the spatial frequency curves produced from images of this area. The curve for image G-5 shows two strong peaks at 90° and 180° that result from N-S and E-W image components respectively. A secondary peak is present at 65° caused by southwest flowing tree-lined streams.

The same area is shown in image G-15 (Figure 10b), recorded after a heavy snowfall in northeast Kansas. The snow cover tends to subdue the agricultural patterns produced by fields and roads and as a result, stream patterns are more obvious. The dominant pattern of the streams in this area is to be southeast, and this pattern is portrayed by the orientational curve which has its peaks at 50° and 65° indicative of a southeast oriented linear pattern. The suppressed agricultural patterns fail to register significantly at their usual 90° and 180° locations as a result of the snow.

Image 0-20 (Figure 11) is an area on the western edge of the Ozark Plateau in northeast Oklahoma and southwest Missouri. This area is partially forested with valley bottoms and level uplands being free of trees and snow covered. The larger streams in the region are deeply incised and appear to be fault or joint-controlled. A major fault, the Seneca fault trends southwest-northeast through the sample site at A-A' its traces being expressed by linear stream segments. Other major stream valleys share a similar orientation. In addition, numerous secondary streams are oriented east-west. These two major trends are also expressed by the orientational curve for this area. High values at 115° to 135° reflect the southwest-northeast orientations while peaks at 175° and 25° result from the east-west pattern.

QUANTITATIVE IMAGE ANALYSIS

As mentioned previously, to reduce the amount of information present in the spatial frequency and orientational curves, various data processing schemes were developed to extract feature parameters from them. It was intended that these feature parameters would characterize geologic or physiographic features which gave rise to fluctuations in the curves. To determine how well these feature parameters characterize each sample area, they may be used as inputs to pattern classification algorithms.

For the purposes of this phase of the investigation, the range of spatial frequencies was divided into two bands. Band 1 contains spatial frequencies between 0.0 and 0.9 cycles/km, and band 2 contains spatial frequencies between 1.06 and 2.8 cycles/km. This division essentially separates information due to high frequency fluctuations such as occur in stream patterns in rough terrain, and low frequency information such as occur due to field patterns. This division of frequencies appears to correspond to a natural break at approximately 1 cycles/km.

Similarly, the range of orientational data was divided into four sectors- each corresponding to 40 degrees. Sector 1 provides data on pattern orientations that produce distributions between 25 and 65 degrees clockwise from true north, sector 2: 65-105 degrees, sector 3: 105-145 degrees, and sector 4: 145-185 degrees.

The following are a few examples of the feature parameters that were calculated from the spatial frequency and orientational curves for each of the bands or sectors listed above:

Orientation feature parameters:

DAV = Average value of the curve in a 40^{o} sector

AREA = Area of curve (A) above and (B) below the average in sector

PEAK = Number of peaks or "spikes" in curve in sector

Spatial frequency feature parameters:
(These are derived from the modified spatial frequency curve)

DAV = Average value of curve in each frequency band

AREA = Area of curve (A) above and (B) below the average in band

DARA = Area of curve (A) above and (B) below the value 1.0 in band

SLOPE 2 = Slope of a calculated regression line for curve in band 2.

Each feature parameter for all 80 non-snow and 68 snow sample areas was plotted versus their appropriate sample area category to form histograms for visual evaluation. The histogram for SLOPE 2 is shown in Figure 12. This appears to be the best single feature parameter and represents the relative hign vs. low frequency relationship for a sample area. Considering this, it is not unreasonable to expect SLOPE 2 to distinguish between plains areas of low high frequency content and hills regions with broken topography resulting in greater high frequency content. As can be seen in Figure 12 a decision boundary may be inserted at approximately zero (+.001) which separates the Flint Hills, Red Hills, and Smoky Hills from the rest of the categories. On the basis of this single feature parameter, these three regions can be separated with an accuracy of 92.5% with only 6 incorrect identifications. Figure 13 shows the results of this classification and its relation to the original categorization of the sample areas. Sample sites represented by a square were identified as belonging to the category comprising the Flint Hills, Red Hills, and Smoky Hills; sample sites represented by a triangle were identifiedas belonging to the category comprising the Arkansas Valley Lowlands, High Plains, Osage Plains, Blue Hills and the Glaciated Region. The classification of the Blue Hills region with the plains regions appears to be legitimate because it is a transition region. The Blue Hills surface characteristics are mixed due to the presence of both agricultural and ranching land use.

On the basis of three feature parameters (SLOPE 2, freq. AREA (B), and freq. DARA (B)) the state can be further subdivided into four categories (1-Glaciated Region,High Plains, and Osage Plains; 2-Smoky Hills and Flint Hills; 3-Red Hills; and 4-Arkansas Valley Lowlands and Blue Hills). Using the 80 non-snow sample areas, this classification results in an accuracy of 75% correct. At the time of this writing work is continuing on incorporating more feature parameters into classification algorithms which will provide more detailed discrimination of the physiographic regions.

CONCLUSIONS

Comparison of ERTS-1 images with their respective spatial frequency and orientational curves reveals that preferred orientations of drainage invariably produce recognizable peaks. Such a capability is deemed to be potentially valuable for deciphering orientational information from remotely sensed scenes that may be quite complex or that appear to lack preferred alignments. This information could be an aid to structural studies.

The intensive agricultural land use in Kansas as expressed on ERTS imagery, has a definite affect on spatial frequency results; however, the township and range land system restricts orientation information to the East-West and North-South directions and this can generally be distinguished from information related to stream orientation. The spatial frequency analysis of areas with multiple land survey systems or in highly developed areas with numerous linear cultural features may not reveal much in the way of geologic ground pattern information.

The analysis of snow-covered areas was performed in an attempt to suppress agricultural patterns. However, snow falls were generally light in Kansas during the past winter, and in many cases field patterns were actually enhanced on ERTS-1 imagery due to varying crop and grass heights. The analysis of all four MSS bands in an area of known parallel drainage produced results which substantiated our choice of MSS5 imagery for use in this study. This band was found to display stream patterns more effectively than the other three.

The results of this investigation to date indicate that optical data processing of ERTS-1 images can be used very successfully in identifying large-scale physiographic patterns in the Great Plains region of the United States. It was shown that large scale physiographic patterns were identified easily based on the quantitative analysis of the information derived from the optical processing of the ERTS-A images.

It appears that the band of frequencies between 1.06 and 2.8 cycles/km contain most of the information on the physiographic character of large-scale ground patterns in Kansas, and are most useful for automatic classification. At the same time the orientational data which consistently characterize preferred stream orientations promise to provide increased reliability of classification.

APPENDIX A

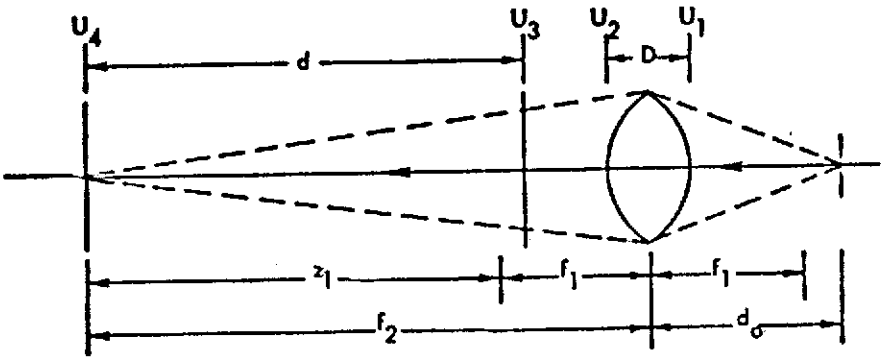

The field distribution U_1 incident upon the lens from the point source d_o in front of the lens can be described using the paraxial approximation for a spherical wave as:

$$U_1(x_1,y_1) = A \exp(jkd_o) \exp\left[j\frac{k}{2d_o}(x_1^2+y_1^2)\right] \quad (1)$$

The field distribution U_2 just behind the lens is given by eqs. 5-2, 5-10, pp. 78-81 from Goodman.

$$U_2(x_2,y_2) = A \exp(jkd_o) \exp(jknD) \exp\left[j\frac{k}{2d_o}(x_1^2+y_1^2)\right] \exp\left[-j\frac{k}{2f_1}(x_2^2+y_2^2)\right] \quad (2)$$

$$= A \exp(jkd_o) \exp(jknD) \exp\left[-j\frac{k}{2}\left(\frac{1}{f_1} - \frac{1}{d_o}\right)(x_2^2+y_2^2)\right]$$

where $x_1 = x_2$, $y_1 = y_2$; and we let $A \exp(jkd_o) \exp(jknD) = A'$

and $\frac{1}{f_1} - \frac{1}{d_o} = \frac{1}{f_2} = \frac{1}{(f_1+z_1)}$ (lens law)

Then

$$U_2(x_2,y_2) = A'\exp\left[-j\frac{k}{2f_2}(x_2^2+y_2^2)\right] \quad (3)$$

This is simply the equation for the field distribution just behind a lens of focal length f_2 when it is illuminated by a normally incident plane wave of amplitude A' delayed by the constant phase $\exp[jk(d_o + nD)]$.

Following the development of Goodman (p. 88) for an object placed behind a lens, the field amplitude transmitted by the image a distance f_2-d behind the lens is

$$U_3(x_3,y_3) = t_o(x_3,y_3)\left\{A'\frac{f_2}{d}P\left(\frac{f_2}{d}x_3,\frac{f_2}{d}y_3\right)\exp\left[-j\frac{k}{2d}(x_3^2+y_3^2)\right]\right\} \quad (4)$$

where: $t_o(x_3,y_3)$ is the transmittance function of the image

$P\left(\frac{f_2}{d}x_3,\frac{f_2}{d}y_3\right)$ is the pupil function of the lens reduced by the ratio d/f_2

And finally the field distribution in the transform plane at a distance $f_1+Z_1 = f_2$ behind the lens is

$$U_4(x_4,y_4) = \frac{A'\exp[j\frac{k}{2d}(x_4^2+y_4^2)]}{j\lambda d}\,\frac{f_2}{d}$$

$$\iint_{-\infty}^{\infty} t_o(x_3,y_3)P(\frac{f_2}{d}x_3,\frac{f_2}{d}y_3)\exp[-j\frac{2\pi}{\lambda d}(x_3x_4+y_3y_4)]\,dx_3\,dy_3 \qquad (5)$$

Thus, aside,from the quadratic phase factor, the amplitude distribution at the transform plane is the Fourier transform of that portion of the object subtended by the projected lens aperture. And, by using a lens of focal length f_1 illuminated by the virtual point source at distance d_o in front, the transform scale is equivalent to that of a lens of focal length f_2 illuminated by a plane wave.

REFERENCES

Andrews, Harry C., et. al., (1972), "Image Processing by Digital Computer," IEEE Spectrum, July, 1972.

Gramenopoulos, Nicholas, (1973), "Terrain Type Recognition Using ERTS-1 MSS Images," ERTS-1 Symposium, March 5-9, 1973, New Carrollton, Maryland.

Goodman, J. W., (1968), Introduction to Fourier Optics, McGraw-Hill Book Co., New York.

Lendaris, G. G. and G. L. Stanley, (1969), "Diffraction-Pattern Sampling for Automatic Pattern Recognition," Seminar Proceedings, Pattern Recognition Studies, Society of Photo-Optical Instrumentation Engineers, June 9-10, 1969, New York.

McCauley, J. R., et. al, (1974), "Stream Pattern Analysis Using Optical Processing of ERTS Imagery of Kansas," Modern Geology, (in Press).

Papoulis, Athanasios, (1962), The Fourier Integral and Its Applications, McGraw-Hill Book Co., New York.

Preston, Kendall, (1972), Coherent Optical Computers, McGraw-Hill Book Co.,New York.

Schoewe, W. H., (1949), "The Geography of Kansas, Pt. 2. Physical Geography," Kansas Acad. Sci. Trans., vol. 52, no. 3, pp. 261-333.

Shulman, A. R., (1970), Optical Data Processing, John Wiley and Sons, Inc.,New York.

Steckley, Robert C., (1972), "Determination of Paleotectonic Principal Stress Direction, Including Analysis of Joints by Optical Diffraction," U. S. Dept. of Interior, Bureau of Mines, PGH., PA. 18036, U. S. Govt. Printing Office: 1972-709-309:551.

Ulaby, F. T. (Principal Investigator), et. al., (1973) "Ground Pattern Analysis in the Great Plains," CRES Technical Report 2266-4," Semi-Annual ERTS-1 User Investigation Report," University of Kansas Center for Research, Inc., Lawrence, Kansas, July, 1973. Supported by NASA Contract NAS5-21822.

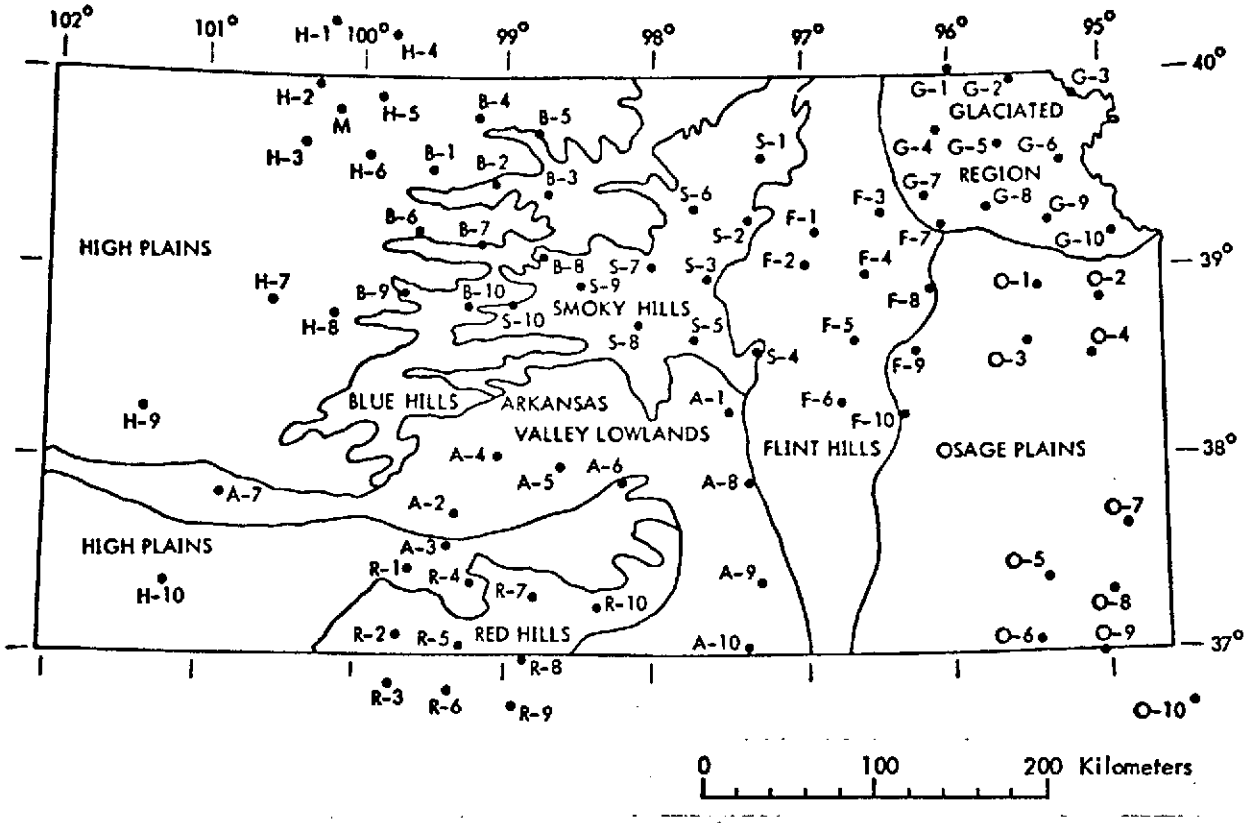

Figure 1. Physiographic Regions of Kansas (Adapted from Schoewe, 1949) with Sample Site Locations.

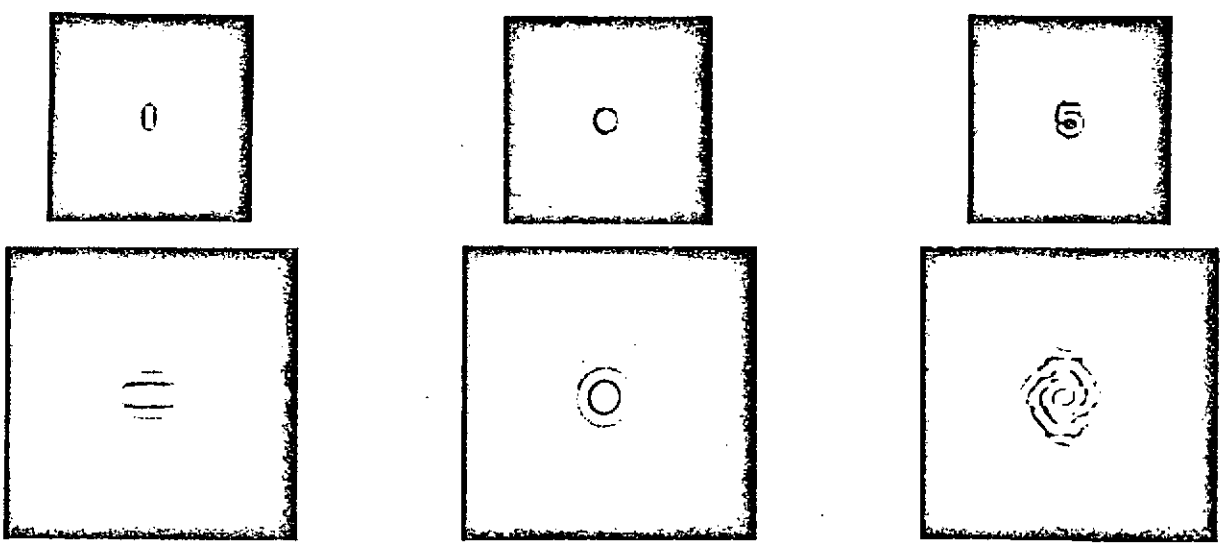

Figure 2. Idealized Transmission Functions and their Optical Diffraction Patterns (Amplitude Frequency Spectra).

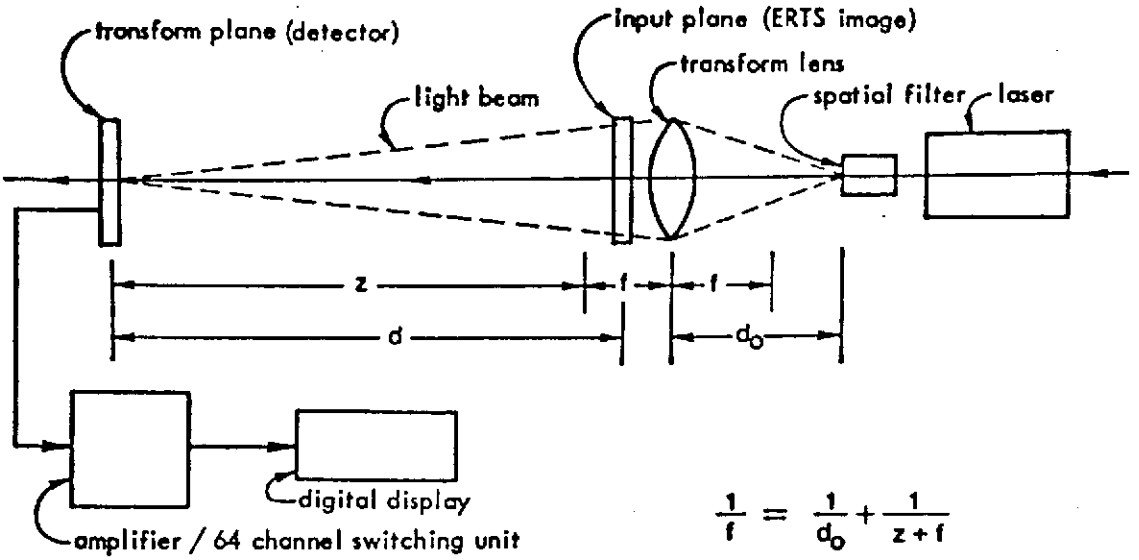

Figure 3. System Configuration.

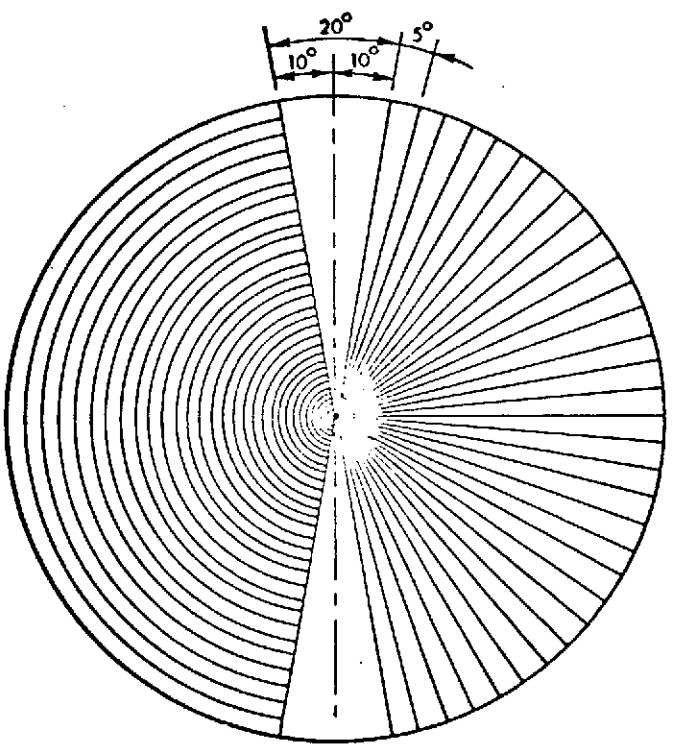

Figure 4. Detector Geometry.

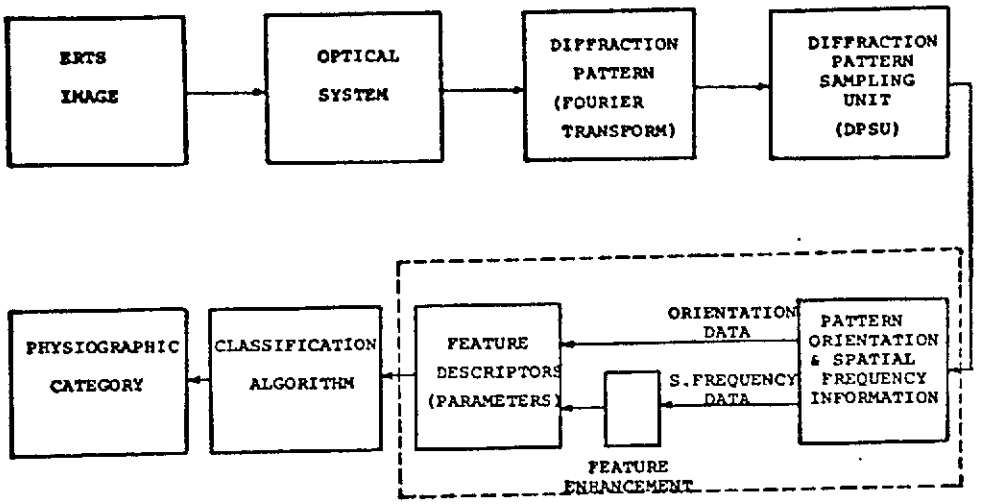

Figure 5a. Block Diagram of Optical Processing and Pattern Recognition System.

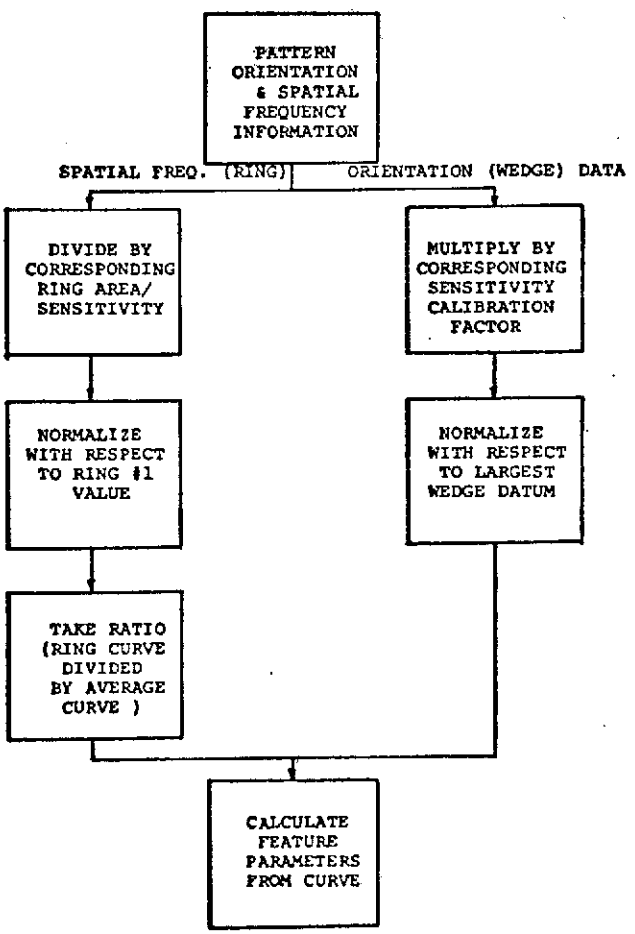

Figure 5b. Detail of Portion of Figure 5a. Enclosed in Dashed Lines.

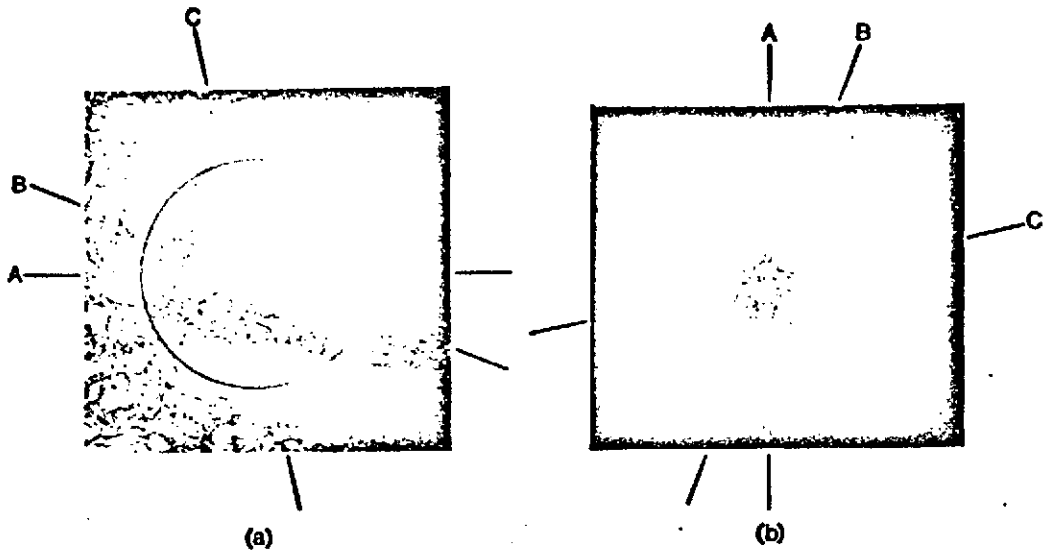

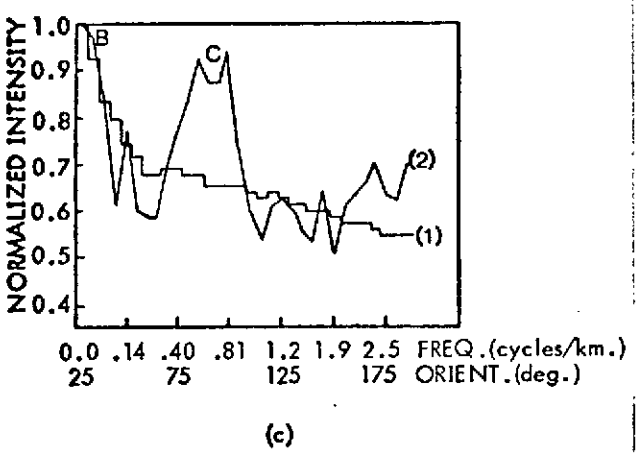

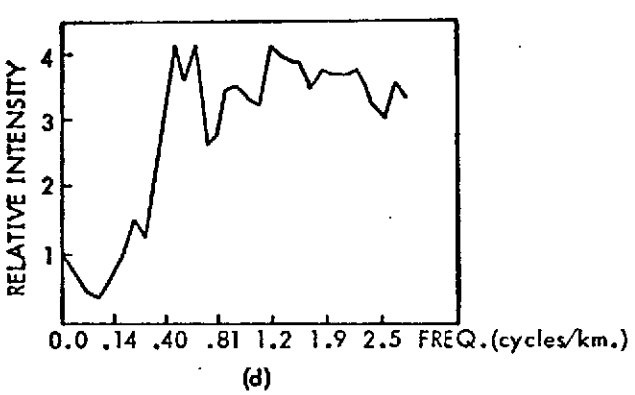

Figure 6. Example Showing Progression of Steps From Portion of ERTS-1 Image No. 1076-16393-5 (6a), to Optical Frequency Spectrum (6b), to Digitized Computer Plots (6c), to modified Spatial Frequency Curve (6d).

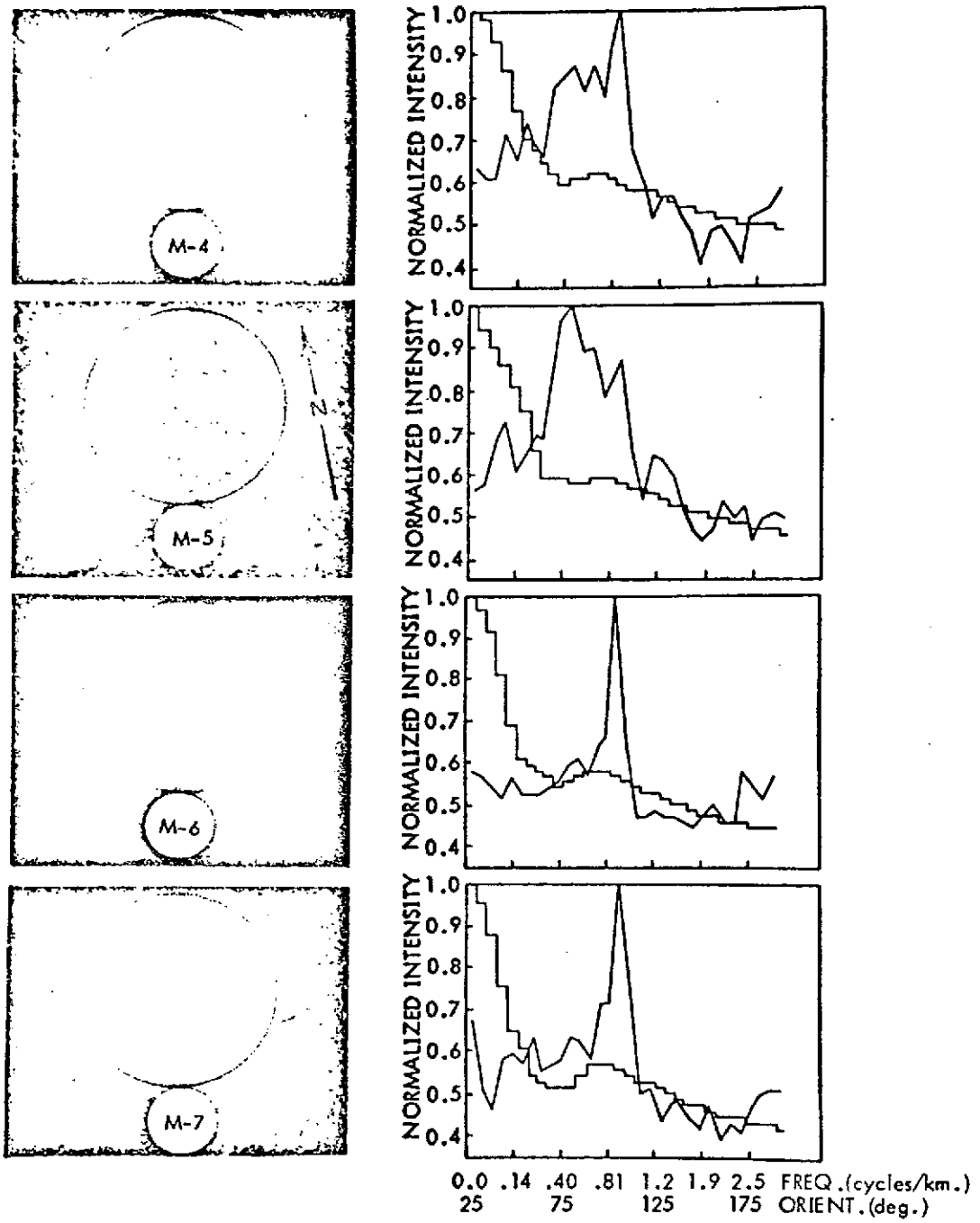

Figure 7. Portions of ERTS-1 Images 1006-16502-4,5,6,7 and Optical Diffraction Curves for Sample M without Snow.

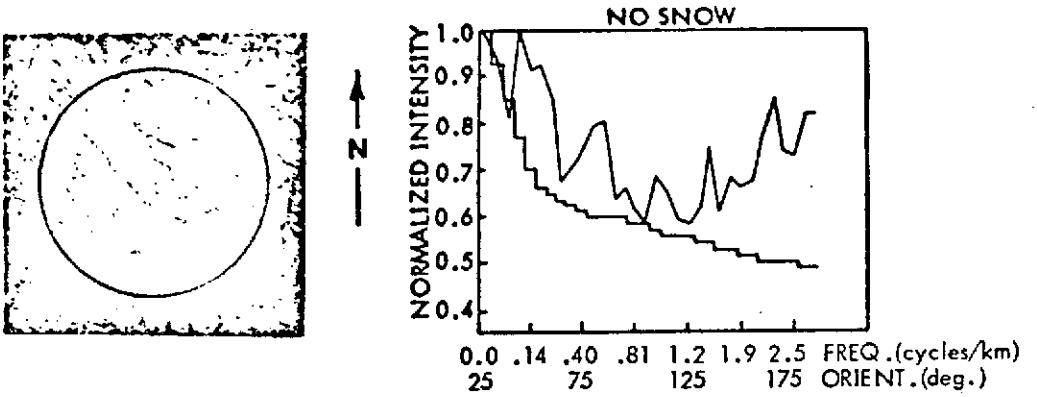

Figure 8. Portion of ERTS-1 Image No. 1076-16393-5 and Optical Diffraction Curves for Sample F-4 without Snow.

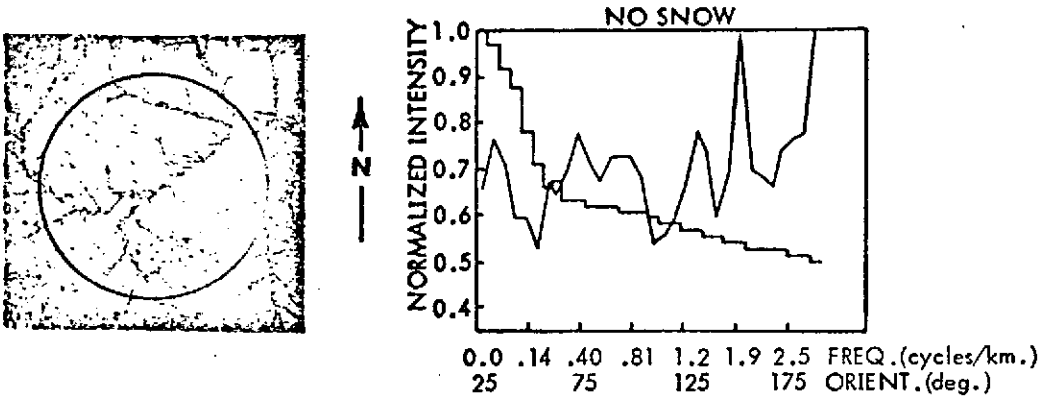

Figure 9a. Portion of ERTS-1 Image No. 1076-16393-5 and Optical Diffraction Curves for Sample F-6 without Snow.

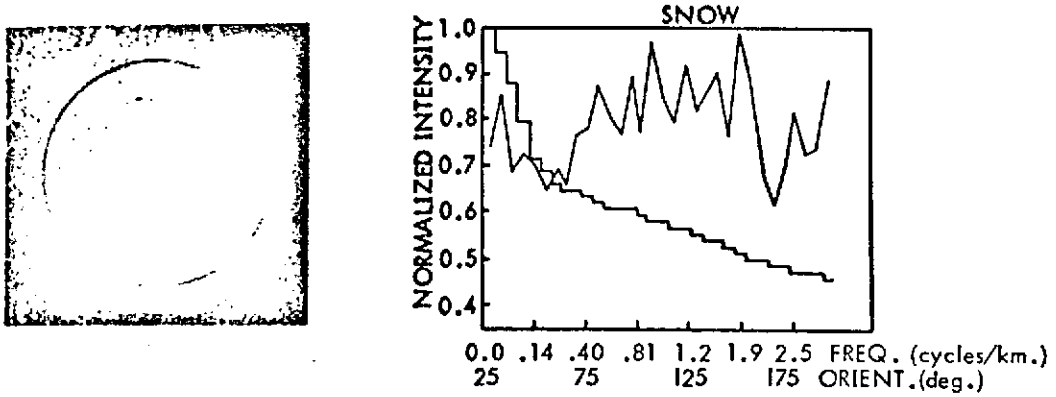

Figure 9b. Portion of ERTS-1 Image No. 1148-16401-5 and Optical Diffraction Curves for Sample F-16 with Snow.

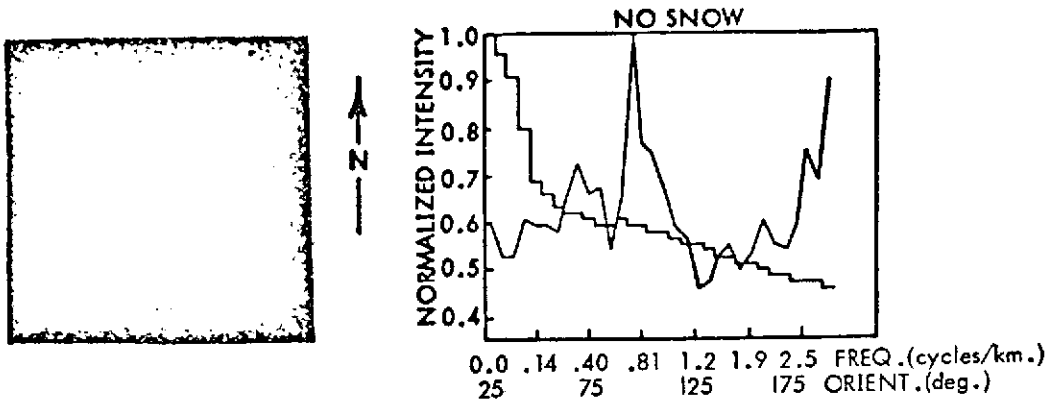

Figure 10a. Portion of ERTS-1 Image No. 1021-16333-5 and Optical Diffraction Curves for Sample G-5 without Snow.

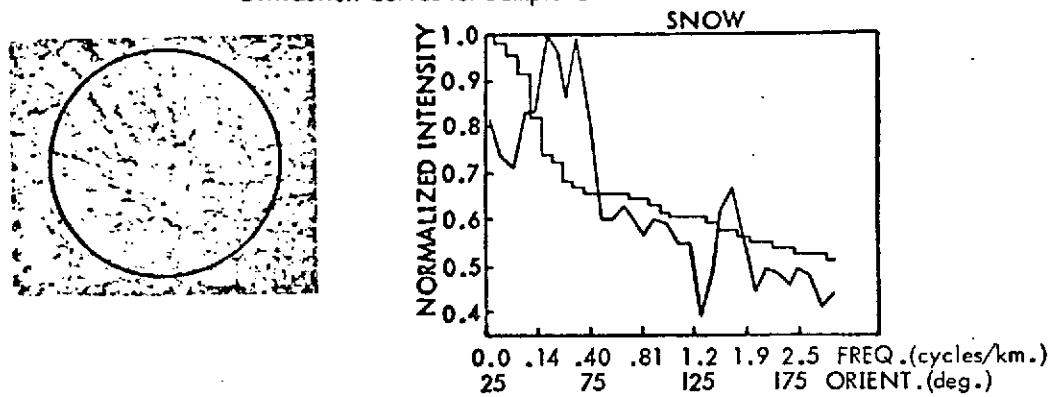

Figure 10b. Portion of ERTS-1 Image No. 1147-16340-5 and Optical Diffraction Curves for Sample G-15 with Snow.

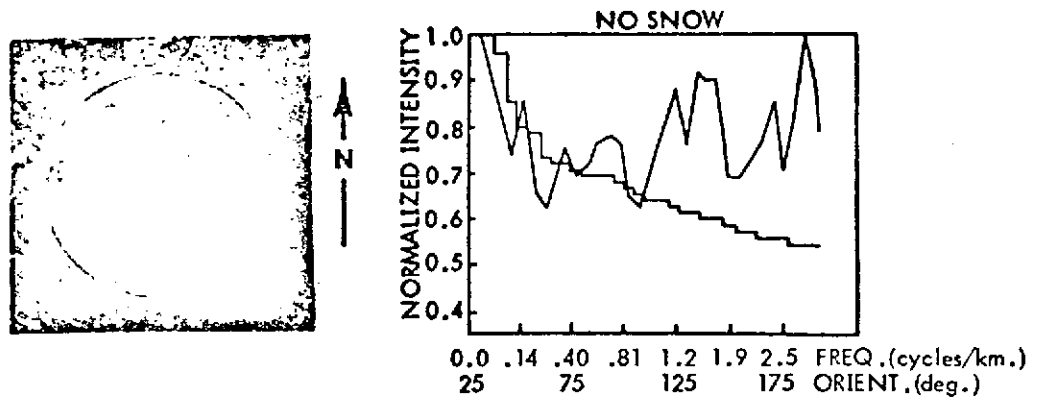

Figure 11. Portion of ERTS-1 Image No. 1146-16291-5 and Optical Diffraction Curves for Sample O-20 with Snow.

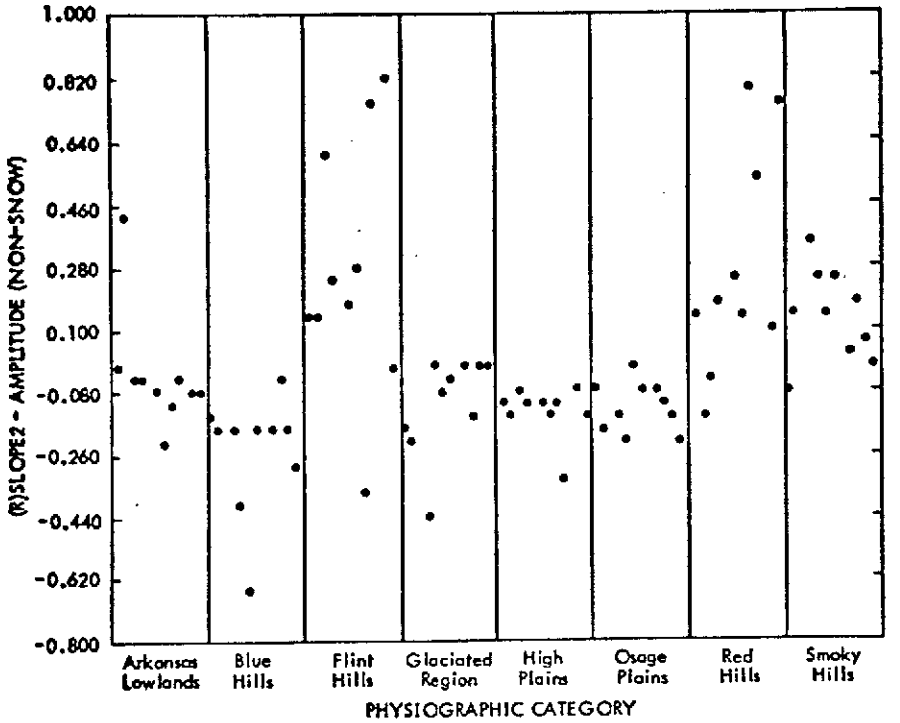

Figure 12. Parameter Plot Using the Parameter SLOPE 2.

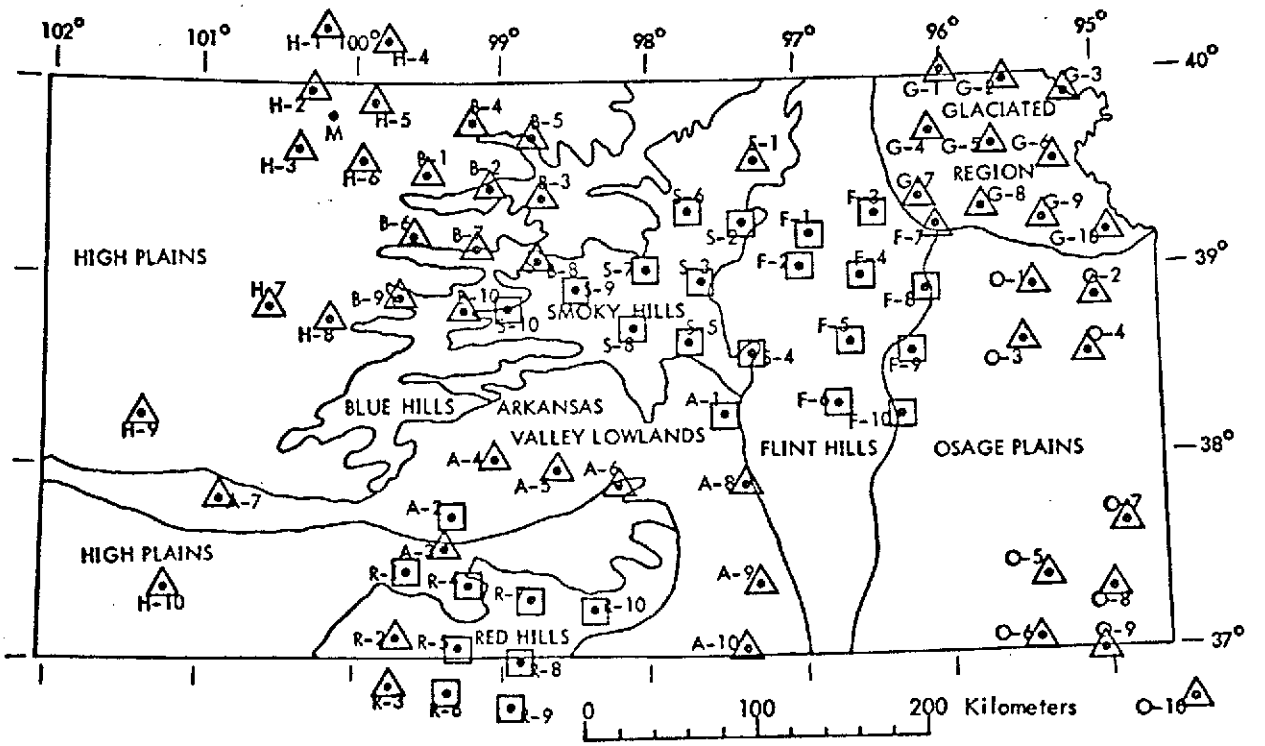

Figure 13. Classification of Sample Areas in Terms of a Decision Made on the Basis of the Value of the Single Parameter SLOPE 2 for Each Sample Area.